ELSEVIER

Polymer 43 (2002) 6829–6837

polymer

www.elsevier.com/locate/polymer

Small angle light scattering investigation of polymer dispersed liquid crystal composites

Jérôme Maugey, Patrick Navard*

Ecole des Mines de Paris, Centre de Mise en Forme des Matériaux, UMR CNRS-Ecole des Mines de Paris No. 7635, BP 207, 06 904 Sophia-Antipolis Cedex, France

Received 27 March 2002; received in revised form 12 August 2002; accepted 19 August 2002

Abstract

The curing of a homogeneous mixture of a nematic liquid crystal and an acrylate UV curable prepolymer was studied by small angle light scattering, varying temperature and UV intensity. For all the conditions except at elevated temperature, the phase separation occurs with a spinodal decomposition which phases can be more or less easily recognised. Whatever the temperature below the clearing point of the liquid crystal and the UV intensity, the isotropic-to-nematic transition that occurs in the liquid crystal rich region is easily seen as a strong decrease of the light scattering intensity. For all the conditions tested, the final morphology is in the form of a droplet morphology. At high UV intensity, there are two scattering peaks that are appearing in the scattering pattern which was tentatively interpreted as a double spinodal decomposition.

Keywords: Small angle light scattering; Polymer dispersed liquid crystal; Phase separation

1. Introduction

Polymer dispersed liquid crystal materials (PDLCs) are composites formed by the dispersion of liquid crystal (LC) droplets in a polymer matrix [1,2]. They are used as display systems in video projection or for electrically controlled light shutters. The basic optical properties of such systems are that their transparency can be electrically modulated. Without any electric field, each LC droplet of the PDLC will scatter the incident light independently because the director in each droplet is not uniform. As a consequence, the cell is opaque. When an electric field is applied, the director in each droplet is oriented. Since the refractive indexes of the liquid crystal and the polymer matrix are matched, the material is then transparent. But the optical properties do not depend only on the choice of the materials, but also on the final structure of the sample (organisation, size, shape). The morphologies are generated during the phase separation from an initially miscible system composed of a prepolymer and a liquid crystal. The technique commonly used for making PDLCs is the polymerisation induced phase separation (PIPS) [3–5]. The increase of the average molar mass of the polymerising prepolymer will induce the phase separation. The final structure is controlled by the competition between the phase separation and the increase of the viscosity of the matrix. At certain point, the matrix vitrifies and the structure is nearly frozen.

This general scheme applies to all materials undergoing a PIPS. When a liquid crystal is involved, one should expect in addition a transition towards a liquid crystalline state since the original mixture is isotropic. This was indeed what was seen in a preliminary work, where a PIPS involving the preparation of a PDLC was studied by small angle light scattering [6]. In this case, not only the isotropic-to-nematic transition was accompanied by a clear scattering sign, but a double spinodal ring was also noted at high curing rate. This preliminary study showed the interest of investigating deeper the phase separation involved in the preparation of PDLC.

For this purpose, the small angle light scattering (SALS) technique is a very efficient method [7–9]. One of the important characteristics of light scattering is that it is a non-destructive test. This makes possible to follow the time-evolution of the phase separation process. The scattering pattern is a direct reflection of orientation, shape and size of the structure. Another advantage is that with an appropriate

* Corresponding author. Tel.: +33-4-93-95-74-66; fax: +33-4-92-38-97-52.

E-mail address: patrick.navard@cemef.cma.fr (P. Navard).

0032-3861/02/$ - see front matter
PII: S0032-3861(02)00568-2

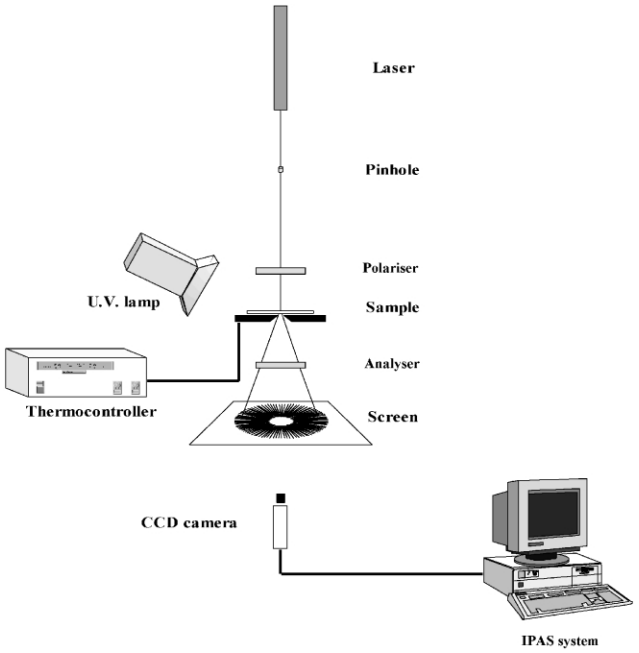

Fig. 1. Optical set-up used to study the evolution of the small angle light scattering patterns with UV irradiation.

choice of instruments, one can follow extremely fast events having a low optical contrast [6,10]. This would be very delicate with only optical microscopy.

In this paper, we will study the phase separation of a mixture comprising an acrylate based UV photocurable prepolymer and a liquid crystal. The phase separation mechanisms are not similar at low and high UV intensities. We will thus describe these two cases in the two main parts of this paper. The goal is to provide a comprehensive picture of how the phase separation proceeds with time and how the final morphology depends on this morphological evolution. As far as possible, the results will be compared with the existing theories.

2. Experimental part

2.1. Materials

The PDLC composite is a mixture of a liquid crystal and a photo-polymerisable resin, both kindly provided by Merck, Pool (UK). The resin called PN 393 is a specially designed acrylate based photocurable system. Its refractive index at room temperature is 1.47. The nematic liquid crystal (TL 205) is a mixture of chloro-terminal groups [11]. Its nematic to isotropic transition temperature is $T_{N-I} =$ 87.4 °C and its birefringence is $\Delta n = 0.2175$.

The results of only one concentration will be reported here, chosen as the one giving the best electrooptical properties.

The initially homogeneous and isotropic mixture of TL 205/PN 393 is prepared by mixing the components at the ratio of 80% of liquid crystal and 20% of prepolymer in weight. A measurement made by an ABBE refractometer gives a refractive index of 1.5575 for a mixture at this concentration.

The phase diagram of the non-polymerised mixture was given by Serbutoviez et al. [12]. Below a certain temperature (13 °C for 80% of TL205 upon cooling), the mixture is phase separated, with droplets of a nematic liquid crystal growing when the temperature is further decreased. Above 13 °C, the two components are miscible. Curing the mixture below 13 °C shows that the nematic droplets do not have a homeotropic configuration at the TL205/PN393 interface. The same microscopy experiments were performed in the homogeneous region (say above 20 °C) during UV curing but were very difficult to interpret.

The mixture was filled by capillary force between two thin glass plates having a spacing of 10 ± 5 μm. This thickness was a compromise, chosen as the largest one keeping multiple scattering effects negligible. Above a 20 μm spacing, multiple are significant (as described in Ref. 13) while below 10 μm, the effect of the walls on the structure will be too large. This effect will be discussed later. Two curing parameters were varied, UV intensity from 0.2 to 4 mW cm^{-2} and temperature from 20 to 100 °C.

2.2. Small angle light scattering

SALS experiments have been performed using a custom made equipment associating an optical set-up and a dedicated software, as illustrated in Fig. 1.

The optical bench is composed of a non-polarised He–Ne laser source (wavelength = 632.8 nm), a UV lamp (UViterno model, wavelength = 365 nm), classical optical devices (polarisers, filters, diaphragm, photodiode, screen, beam-stop) and a CCD camera. Two optical configurations will be considered. The sample will either be placed under a non-polarised configuration or between crossed polarisers (depolarised light), whether the purpose is to investigate the concentration fluctuations or the anisotropy fluctuations. The acquisition system is protected by a black box. A thermoregulator device (LINKAM THMS 600) keeps the sample at the curing temperature, fixed by a thermocontroller (LINKAM TMS 91). For low temperatures, the thermocontroller is coupled with a cooling system using liquid nitrogen.

The dedicated software is called IPAS [14]. It allows a very fast and precise analysis of light scattering patterns. The system has more than fifty functions allowing an automatic analysis of most of the classical light scattering patterns. For our case, where a very fast phase separation takes place, the scattering patterns were first recorded on a video tape, then analysed by IPAS. Each image was coded with a timer. Since all the light scattering patterns observed had a circular symmetry, an averaging of the patterns over 360° was made in order to increase the signal/noise ratio. In the following, the scattering intensity is given versus the

Table 1
Start time of phase separation as seen by SALS versus UV intensity

I_{UV} (mW cm^{-2})	0.2	0.65	1.0	1.25	1.70	2.20	2.90	4
t_s (s)	5.33	5.16	3.25	2.44	2.66	1.56	1.70	0.6

polar diffusion angle, θ, that is linked to the scattering wavevector q by:

$$q = \frac{4\pi}{\lambda}\sin\frac{\theta}{2}$$

3. Results and discussion

As a general and common feature, the larger is the UV intensity, the faster is the curing. At 25 °C, the first detectable SALS signal is occurring at a time noted ts after the start of irradiation. ts varies from 5 to 0.6 s, varying UV intensity from 0.2 to 4 mW cm^{-2}, respectively. Table 1 gives the variation of ts with the UV intensity. ts is not continuously decreasing with UV intensity because of the variation of the sample thickness. ts is not also an absolute measurement of the beginning of the phase separation, since it is technique and sensitivity dependent. Other values of ts would be found by other measurement techniques having different observation windows [15].

As already said in Section 1, there are two different morphology evolutions depending on the UV curing intensity. Below a threshold that is around 1 mW cm^{-2}, the evolution is characterised by the appearance and the complex evolution of one single scattering ring. Above 1 mW cm^{-2}, the SALS pattern shows two scattering rings.

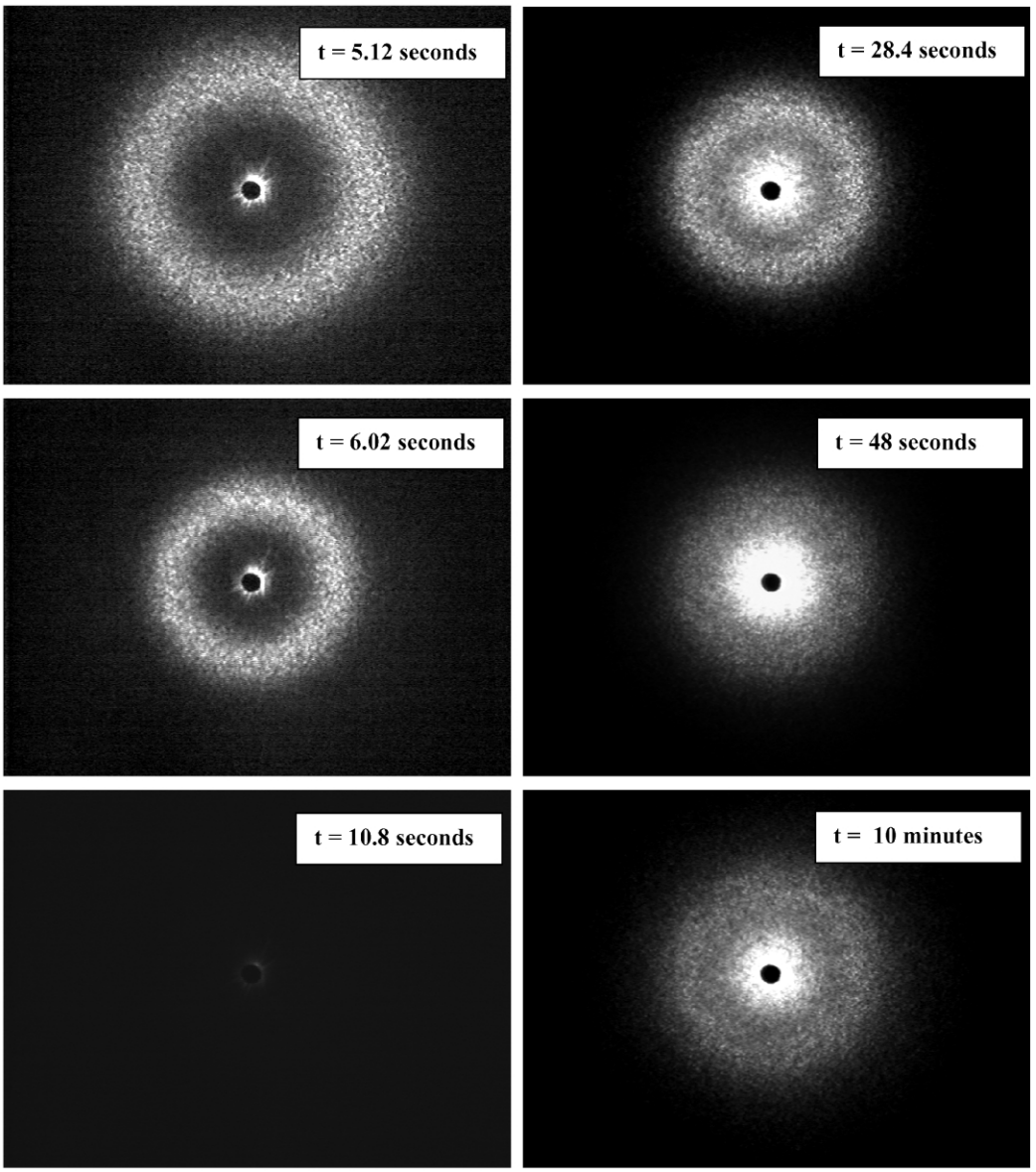

Fig. 2. Evolution of the unpolarised scattering patterns for a sample cured at 25 °C under 0.2 mW cm^{-2}.

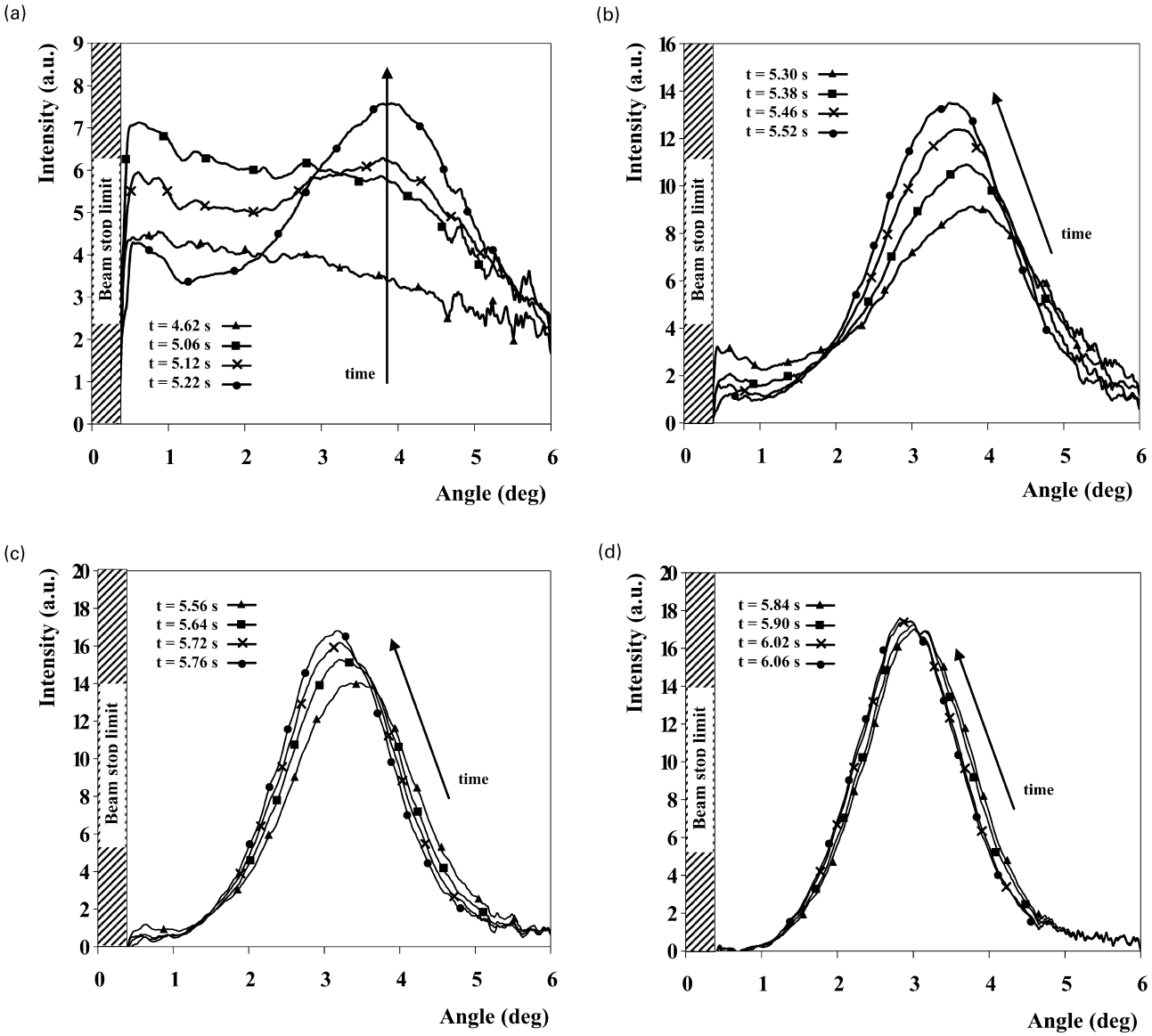

Fig. 3. Phase 1 (low UV irradiation). Intensity of the scattered light as a function of scattering angle. (a) ts from 4.62 to 5.22 s. (b) ts from 5.30 to 5.52 s. (c) ts from 5.56 to 5.76 s. (d) ts from 5.84 to 6.06 s.

This difference lies in the competition between reaction velocity and diffusion coefficients of the different species. We will thus in the following consider first the low irradiation intensity, then the high irradiation intensity.

3.1. Low UV intensity curing

As the sequence of morphological events is the same for all the irradiation intensities below 1 mW cm^{-2}, we will describe in details the SALS results for one intensity, 0.2 mW cm^{-2} at the temperature of 22.5 °C. At low UV radiation, the phase separation is rather a slow process. One can estimate that the morphology is nearly frozen after 10 min. In the following, we will describe step by step the major events encountered. A conclusion will be given at the end of each step. Non-polarised and depolarised light will be simultaneously considered. The evolutions of the scattering patterns are given in Fig. 2.

After five seconds, a clear ring appears. The ring moves to smaller scattering angles with time and five seconds later, the scattering is completely disappearing, the sample being fully transparent. This very puzzling phenomenon will be explained later. The ring then reappears 10 s later together with a halo that will fill the whole scattering pattern at about ts = 40 s. This halo will slowly disappear to leave a ring, as the final SALS pattern. Three phases can be clearly identified.

Phase 1

($t = 0–6.06$ s) is the location of a spinodal decomposition phase separation, where the different stages can be clearly identified.

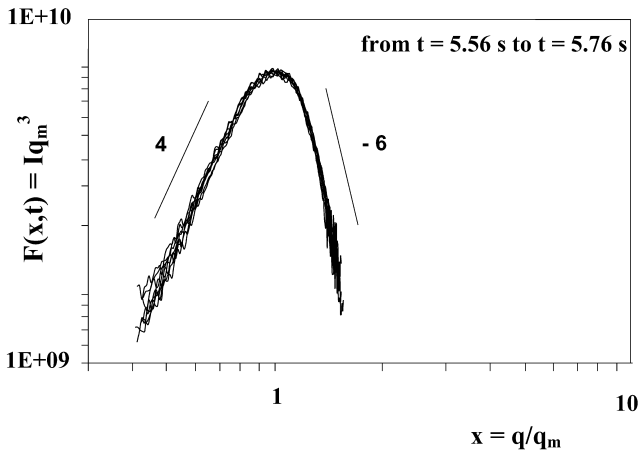

Fig. 4. Superposition of all the curves from ts = 5.56 to 5.76 s (taken every 1/25 s), and plotted as $F(x,t)$ (see text) versus q/q_m, q being the scattering vector and q_m, the scattering vector where the scattering intensity is maximum.

Phase 2
($t = 6.06–19.02$ s) is where the isotropic-to-nematic transition takes place.
Phase 3
($t = 19.02$ s to $t = 10$ min) is where co-continuous structure due to the spinodal decomposition is fragmenting into droplets.

These three phases are described in more detail below.

3.1.1. Phase 1 (ts = 0–6.06 s)

The first unpolarised light scattering pattern appears after 5.12 s. It is a very clear, single ring. The centre of the image around the beam-stop is completely dark. Then, the ring brightens and moves to smaller scattering angles as the phase separation proceeds. Its intensity reaches a maximum at ts = 6.06 s.

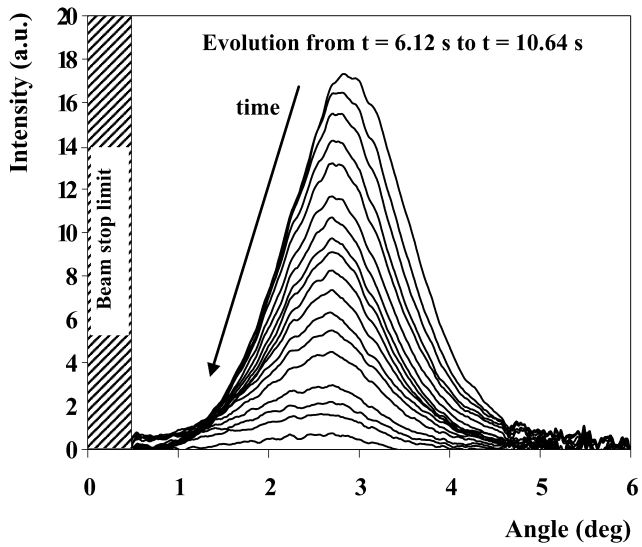

Fig. 5. Phase 2 (low UV irradiation) Scattering intensity versus scattering angle (ts = 6.12–10.64 s).

The depolarised light patterns are very weak, with a pattern appearing after 5.5 s, a short time after the one observed under non-polarised light. This difference is due to the very small intensity of the scattered light. It is a faint halo that shrinks to small angles while increasing its intensity increases and reaching a maximum at the same time as the unpolarised light (6.06 s). The origins of the weak depolarisation are the depolarisation due to the interfaces and the probable fact that small regions may already be in a nematic state due to concentration variations. Macroscopically, the system is isotropic in this first stage.

Fig. 3a–d show the unpolarised scattering intensity variation as a function of scattering angle. A peak can be distinguished at ts = 4.62 s and very clearly seen at 5.12 s. Fig. 3 show the first stages of a typical spinodal decomposition [16–18]. First, the peak grows at a fixed scattering angle (early stage, Fig. 3a). Then its intensity continues to grow and it moves to smaller scattering angles (Fig. 3b, intermediate stage). Two late stages can be identified, noted I (Fig. 3c) and II (Fig. 3d).

The first two stages are typical of a spinodal decomposition. In the late stage of a spinodal decomposition, the self-similarly growth of the morphology is described by Binder and Stauffer [19]. In this case, it is useful to define a scaled structure factor $F(x,t)$ in the following way [20,21]:

$$F(x,t) = I(q,t)q_m^d(t)$$

where $x = q/q_m(t)$ and $d = 3$ for a three-dimensional system. q_m is the scattering wavevector of the dominant mode of the concentration. In this late stage, $F(x,t)$ must be independent of time. We observe such a result (Fig. 4) in the time range 5.56–5.76 s, that we called late stage 1 (Fig. 3c). This is also in agreement with the theoretical scaling functions predicted by Furukawa [22,23] for self-similar co-continuous percolated structures. For $x < 1$, the x^4 dependence is in agreement with published experimental results [24–26] involving weak thermal force contributions. For $x > 1$, the -6 exponent is typical of a thermally quenched critical binary mixture.

However, after ts = 5.80 s, $F(x,t)$ is no more independent of time. This is why we called this period the late stage 2 (Fig. 3d). It has to be noted that the theoretical approach described above is only valid in the case, where the phase separation does not involve a chemical reaction, like the polymerisation of one of the components of the mixture. This is obviously not our case and this is explaining why it is not working over the whole final curing stage. In our case, the polymerisation of PN393 increases the viscosity of the blend and slows down the evolution of the morphology.

3.1.2. Phase 2 (ts = 6.06–19.02 s)

After 6.06 s, the peak continues to evolve to small angles, but its intensity drops down up to zero intensity (Fig. 5). This is very peculiar and not in apparent agreement with a classical spinodal decomposition process. When the peak

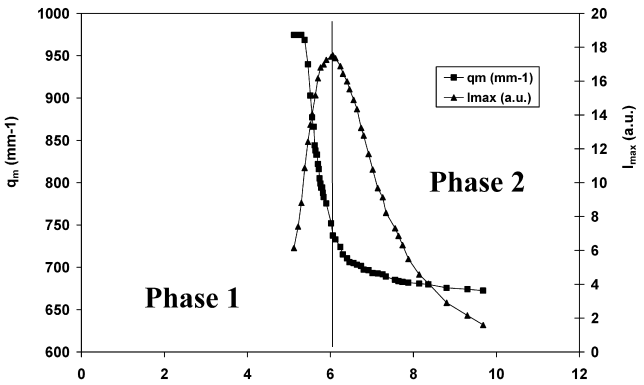

Fig. 6. I_{max} and q_m for step 1 and step 2 of the phase separation. The sample is cured at 25 °C under 0.2 mW cm^{-2}.

disappeared, its angular position was 2.6°. The evolution of the maximum intensity I_m and the scattering vector of the peak maximum q_m in Phases 1 and 2 are given in Fig. 6 as a function of time. The disappearance of the scattering intensity is associated with an increase of the intensity at zero angle, showing that the sample became fully transparent. This can be understood by considering that this is the point, where the composition of the phase rich in liquid crystal reaches the isotropic-to-nematic transition. In our experimental set up, the phase transition is not homogeneous through the thickness of the sample, even if the spacing is small. The phase transition is more advanced near the upper glass plate, close to the UV lamp. At that point, the orientation is generated at the wall interface, and propagates inside the sample with the isotropic–nematic transition. We observed by looking at the behaviour of the pure nematic fluid that it is homeotropically oriented near a glass wall. The sequence of events is thus the following. As soon as the region close to the upper wall and rich in liquid crystal becomes nematic, it orients in homeotropic configuration. This configuration propagates inside the sample since more regions turn nematic. At the end, all the LC rich regions are nematic, all oriented in the homeotropic configuration, i.e. with the director along the laser beam. The principle of PDLC is that in this case (addressed PDLC), the system is transparent (the ordinary refractive index of the liquid crystal matches exactly the refractive index of the polymer. There is no more light scattering. This is happening only when the spacing is small. With a gap of 15 μm, there is a decrease of scattering intensity, but not its disappearance.

3.1.3. Phase 3 (ts = 19.02 s to ts = 10 min)

After 19.2 s, a pattern reappears. It is a ring, but now there is a bright halo around the beam-stop. This halo grows up with time and overcome the ring. Its intensity then slowly decreases and at the end of the experiment, the ring is again clearly observable (Fig. 7), at a polar angle of 2.6°.

The halo seen in unpolarised light configuration is associated with a four lobe pattern in the depolarised configuration (Fig. 8). This pattern remains present until the

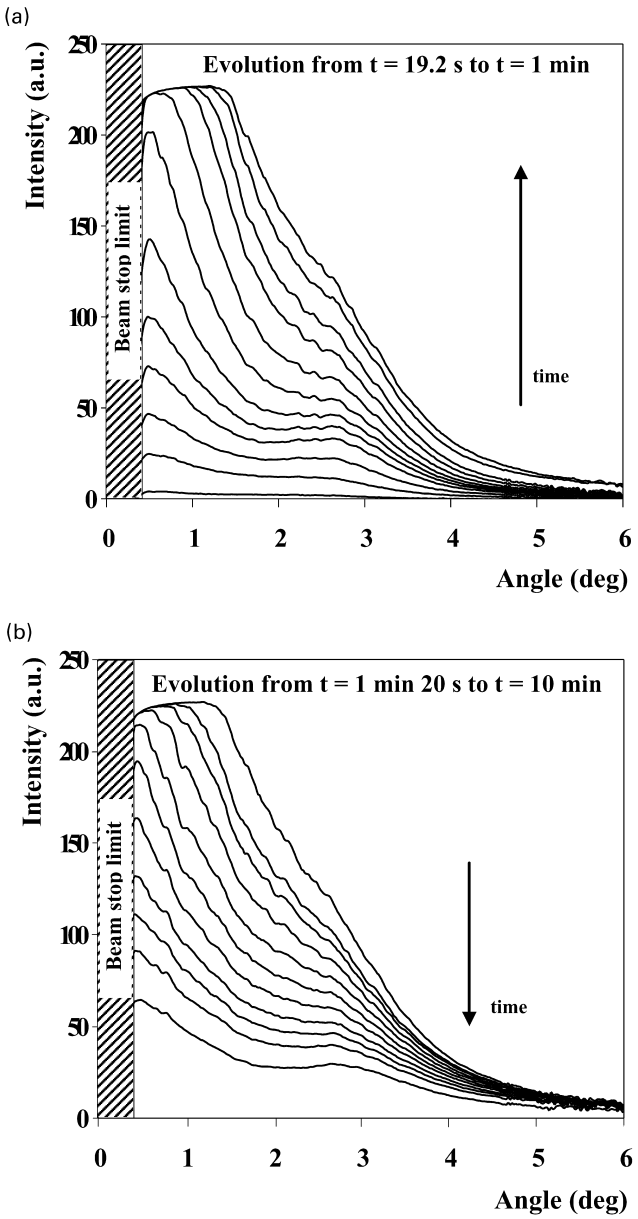

Fig. 7. Phase 2 (low UV irradiation) Scattering intensity versus scattering angle (ts = 6.12–10.64 s) (a) ts from 19.2 s to 1 min (b) ts from 1 min 20 s to 16 min 40 s.

end of the experiment. The scattering maximum is located along a 45° azimuthal angle and the corresponding θ_m is measured equal to 2.6°.

The very high interfacial energy generated by the co-continuous structure leads to the breakage of this structure into droplets, if the structure is not frozen by crystallisation or glass transition. This is what is occurring here. When the structure breaks down, two events change the director orientation. First the co-continuous structure transforms into droplets, where a homogeneous director orientation cannot exist. Second, as can be seen on the large droplets that form at low temperatures, the director tends to orient parallel to the walls formed by the polymer. All this gives rise to bipolar droplets, as for the case of the curing in the phase

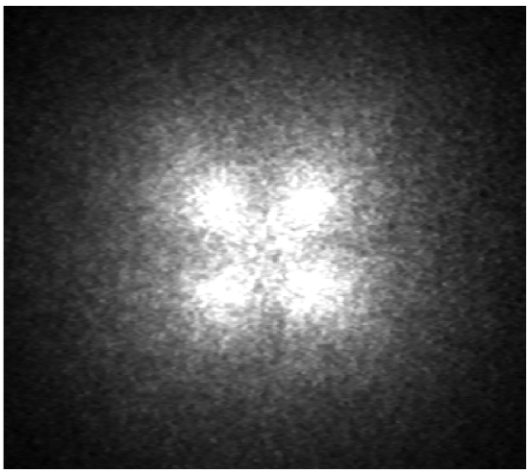

Fig. 8. Four lobe pattern observed between crossed polarisers. Sample cured at 25 °C under 0.2 mW cm^{-2} of UV irradiation.

separated region, at low temperatures. Coming from a spinodal structure, the droplets will be fairly monodispersed in size and regularly dispersed [27]. The mean distance between droplets can be estimated as being equal to the wavelength of the concentration fluctuation before the breakage. This gives about 13.9 μm using Bragg's law. The four lobe depolarised pattern confirms the presence of spherical droplets [28]. The angular position of the scattering maximum can give an estimate of the sphere diameter. For bipolar droplets Ding and Yang [29] calculated the value of U_m if the director is parallel (U_m = 3.86) or perpendicular (U_m = 4.68) to the laser beam, U_m being given by

$$U_m = \frac{4\pi\bar{R}}{\lambda_m}\sin(\theta_m/2)$$

With λ_m the wavelength of light in the medium, θ_m the scattering angle at the maximum intensity. Since the droplets comes from a structure with the director in the laser direction (this was the reason why the scattering vanishes at the isotropic–nematic transition), the bipolar droplets will have also their axis parallel to the laser beam. This gives a mean droplet radius of 8.5 μm (± 1.2 μm). This value is compatible with the Bragg distance Λ calculate from the angular position of the unpolarised ring assuming a compact arrangement ($\Lambda = R\sqrt{3}$ = 14.7 μm compared to Λ = 13.9 μm measured).

3.1.4. Effects of temperature and UV intensity

For a UV intensity of 0.2 mW cm^{-2}, the scattering pattern evolution follows what has been described above up to a temperature of 30 °C. Above 30 °C, it is a halo, not any more a ring, that moves to smaller scattering angles. Its intensity decreases strongly at the isotropic–nematic transition, but without disappearing like below 30 °C. The four lobe HV pattern is present up to 84 °C, above which the whole system is isotropic, being above the clearing point of the liquid crystal. In fact, the clearing point of the pure

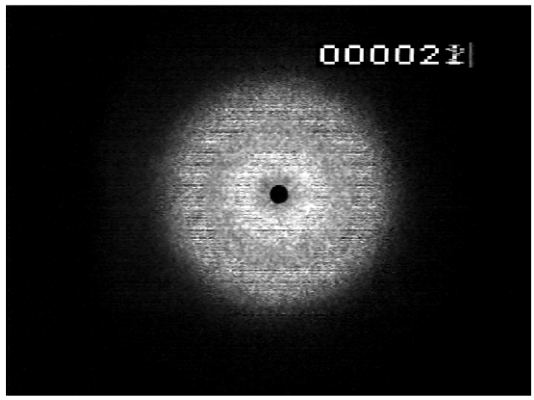

Fig. 9. Unpolarised light scattering pattern obtained at 22.5 °C for 4 mW cm^{-2}.

liquid crystal is slightly higher. The difference may be due to the presence of a small fraction of monomer dissolved in the LC phase.

3.2. High UV intensity curing

We report here the results obtained for UV irradiations larger than 1 mW cm^{-2}. We choose as an example 4 mW cm^{-2}, which is close to the UV intensity used to prepare PDLC cells. Two ranges of temperature can be identified.

Above about 26 °C, the SALS pattern is a wide halo that moves to small angle rapidly, with a sudden increase of the unscattered beam at ts = 2–3 s depending on the temperature. This corresponds to the isotropic-to-nematic transition. At this high UV intensity, the nematic regions have no time to be in an homeotropic configuration. At about ts = 6 s, the scattered intensity around the incident beam decreases and a ring appears. When the depolarised configuration is used, there is a four lobe instead of a ring. This final morphology is somehow similar to what was obtained for low temperatures at low UV intensity. The main spacing between spheres is 12 μm at 26 °C, 8.8 μm at 28.5 °C and 8 μm at 35 °C.

Below 26 °C, the SALS patterns show a very different behaviour. As an illustration, we will give the results obtained at a temperature of 22.5 °C. The first observation is that the SALS pattern appears in the form of two rings, as illustrated in Fig. 9 and noted 1 and 2 on Fig. 10a. Soon after their appearance, the ring 1 at lower scattering angle moves to small angles. At ts = 1.28 s, this ring disappears in the beam stop up to ts = 1.34 s, where a sudden high intensity scattering, staying 0.2 s, blurs the pattern. The final pattern is a halo plus a weak ring at high scattering angle (Fig. 10b). In the depolarised configuration, the first scattering pattern is a weak halo which is increasing or decreasing its intensity as is doing the unpolarised scattering. At no time can a four lobe pattern be found.

These results suggests that the phase separation is initiated by a spinodal process. The presence of two rings

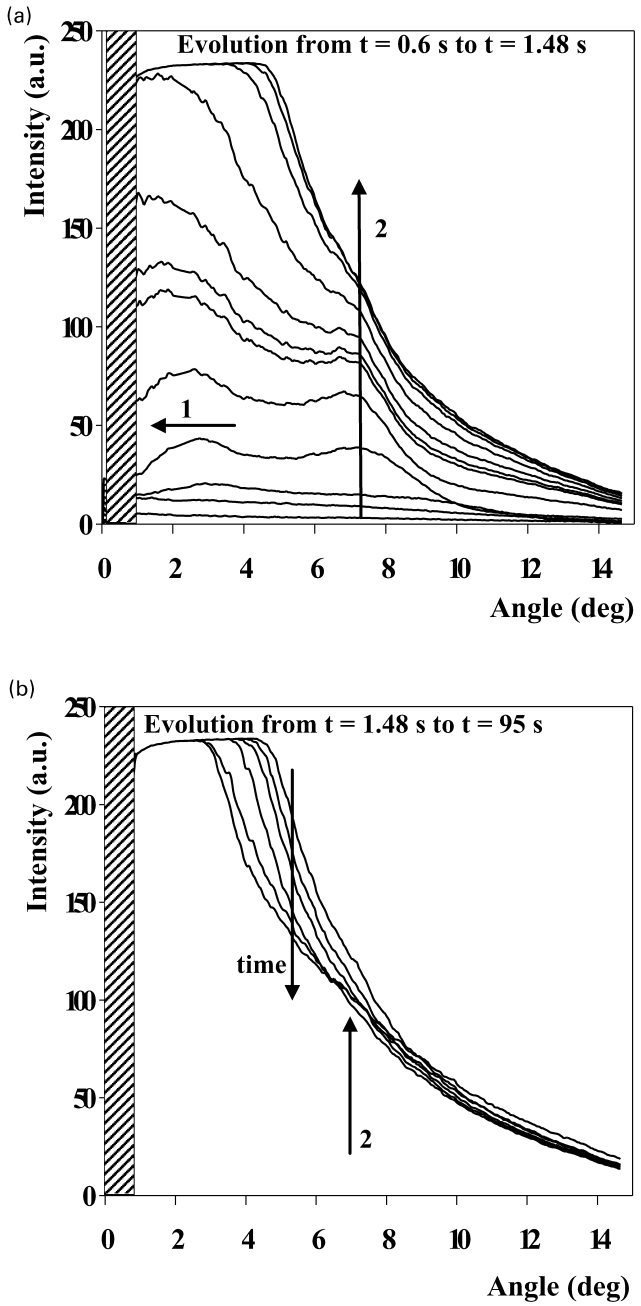

Fig. 10. Scattering intensity versus scattering angle at 4 mW cm^{-2} (T = 22.5 °C). (a) ts = 0–1.48 s (around 100 ms between two curves). The two peaks are clearly seen. (b) ts from 1.6 to 95 s. The peak around 7° is hardly visible.

is rather unusual. A possible explanation is that due to the high UV intensity and thus the quick kinetics of the phase separation, the diffusion of species is slowed down by viscosity. The system is then in a deep non-equilibrium state that may drive two spatial phase separations, one at a large scale, one at a much local scale. There would thus be two spinodal processes, one occurring inside the small domains of the large scale structure. The fact that the size of the large scale structure increases and not the small scale one is a bit puzzling. One should expect the structure at lower scale to be the easiest to change its scale since the diffusion distances are small. Its associated ring at high scattering angle cannot be a second order scattering, since it is as a fixed position, while the first order is moving. Another explanation is that there is a formation of small droplets of polymer inside the LC rich phase that are close enough to give a coherent scattering ring. The fact that we do not see a four lobe pattern is not in agreement with this hypothesis (an isotropic drop inside a LC matrix is scattering as a LC drop inside an isotropic matrix and thus should give rise to a strong depolarised four lobe pattern). This interesting phenomenon, ascribed tentatively to a double spinodal decomposition, is occurring in fast curing systems, and may be commonly encountered with mixtures that are quenched rapidly.

4. Conclusion

The formation of phase-separated morphologies in fast curing LC-thermoset mixtures can be easily studied by SALS. The PN393–TL205 mixtures show that the isotropic-to-nematic transition can be seen as a decrease of the scattering intensity. The morphological changes during curing are complex and fast, changing sometimes in less than 0.5 s. Most features can be interpreted without difficulties. The peak at large scattering angle that is formed when the UV intensity is large has not been clearly understood. This unusual phenomenon may deserve more structural analysis.

References

[1] Doane JW, Vaz NA, Wu BG, Zumer S. Appl Phys Lett 1986;48(4):269–71.
[2] Drzaic PS. Liquid crystal dispersions. Series on liquid crystals, vol. 1. Singapore: World Scientific; 1995.
[3] Oh J, Rey AD. Comput Theor Polym Sci 2001;11:205–17.
[4] Oh J, Rey AD. Macromol Theor Simul 2000;9:641–60.
[5] Vaz NA, Smith GW, Montgomery GP. Liq Cryst 1987;146:1–15.
[6] Maugey J, Budtova T, Navard P. In: te Nijenhuis K, Mijs W, editors. The Wiley polymer networks review, vol. 1. New York: Wiley; 1998.
[7] Kyu T, Mustafa M, Yang JC, Kim JY, Palffy-Muhoray P. In: Noda I, Rubingh DN, editors. Polymer solutions, blends and interfaces. Amsterdam: Elsevier; 1992. p. 245.
[8] Kim BS, Chiba T, Inoue T. Polymer 1995;36:67–71.
[9] Okada M, Fujimoto K, Nose T. Macromolecules 1995;28:1795–800.
[10] Sondergaard K, Lyngaae-Jorgensen J. Rheo-physics of multiphase polymer systems. Lancaster: Technomic; 1995.
[11] Trubert C. Modélisation et caractérisation des composites polymère/cristal liquide en vue de leur application aux écrans plats. Thèse de doctorat. France: Université de Rennes I; 1995.
[12] Serbutoviez C, Kloosterboer JG, Boots HJM, Paulissen FAMA, Touwslager FJ. Liq Cryst 1997;22(2):145–56.
[13] Maugey J, Van Nuland T, Navard P. Polymer 2002;42:4253–66.
[14] IPAS is commercialised by Laser Instrument Diffusion, 495 route de la mer, 06410 Biot, France.
[15] Girard-Reydet E, Sautereau H, Pascault JP, Keates P, Navard P, Thollet G, Vigier G. Polymer 1998;39(11):2269–79.

[16] Chen W, Kobayashi S, Inoue T, Ohnaga T, Ougizawa T. Polymer 1994;35(18):4015–21.
[17] Hashimoto T. In: Thomas EL, editor. Material science and technology. Structures and properties of polymers, vol. 12. Weinheim: VCH; 1993. p. 251–300.
[18] Lal J, Bansil R. Macromolecules 1991;24:290–7.
[19] Binder K, Stauffer D. Phys Rev Lett 1974;33:1006.
[20] Gunton JD, San Miguel M, Sahni PS. In: Domb C, Lebowitz JL, editors. Phase transition and critical phenomena, vol. 8. New York: Academic Press; 1983.
[21] Kim JY, Cho CH, Palffy-Muhoray P, Mustafa M, Kyu T. Phys Rev Lett 1993;71(14):2232–5.
[22] Furukawa H. Physica A 1984;123:497.
[23] Furukawa H. J Phys Soc Jpn 1989;58:216.
[24] Takenaka M, Hashimoto T. J Chem Phys 1992;96:6177.
[25] Lauger J, Lay R, Maas S, Gronski W. Macromolecules 1995;28: 7010–5.
[26] Takenaka M, Izumitami T, Hashimoto T. J Chem Phys 1993;98:3528.
[27] Inoue T. Prog Polym Sci 1995;20:119–53.
[28] Van de Hulst HC. Light scattering by small particles. New York: Wiley; 1957.
[29] Ding J, Yang Y. Mol Cryst Liq Cryst 1994;257:63–87.